Low field magnetocaloric effect of PrCo3 compounds

W. Bouzidi, K. Nouri, T. Bartoli, H. Jaballah, S. Ayadim, J. Moscovici, Lotfi Bessais

Low Field Magnetocaloric Effect of $PrCo_3$ compounds

W. Bouzidi,[1] K. Nouri,[1] T. Bartoli,[1] H. Jaballah,[2,3] S. Ayadim,[2] J. Moscovici,[2] and L. Bessais[2,*]

[1] *Capgemini Engineering, Direction Research & Innovation Department, 2 rue Paul Dautier, 78140, Vélizy-VillaCoublay, France*

[2] *Univ Paris Est Creteil, CNRS, ICMPE, 2 rue Henri Dunant F-94320 Thiais, France.*

[3] *Université de Tunis El Manar, Faculté des Sciences de Tunis, Lab Mat Org & Propriétés LR99ES17, Tunis 2092, Tunisia.*

(Dated: October 11, 2023)

Rare-earth-transition-metal intermetallics show very interesting magnetic properties for numerous applications (hard magnetic materials, magnetic refrigeration ...). This paper is devoted to the study of the structural, magnetic and magnetocaloric effect (MCE) of the intermetallic nanomaterials $PrCo_3$, which derives from the $PuNi_3$ type structure. This system crystallizes into the rhombohedral structure ($R\bar{3}m$ space group). $PrCo_3$ compound exhibits a second order ferro - paramagnetic transition at around 330 K. This 1:3 system, based on a stacked Pr_2Co_4 and $PrCo_5$ units, has a magnetocaloric effect of 1.3 J/kg K at low field. In addition, we demonstrated that the MCE derived from phenomenological and experimental approaches were in agreement.

PACS numbers: 75.50.Bb, 75.50.Tt, 76.80.+y

I. INTRODUCTION

Rare-earth-transition-metal ($R-T$) intermetallic alloys are generally characterized by a high magnetic transition temperature and a single-axis (uniaxial) anisotropy. In addition, for a well optimized microstructure, they can show a high coercivity [1–3].

Several studies have focused on the magnetic properties of $4f$ rare-earth (R) and $3d$ transition metal-based (T) intermetallics, both for their interesting magnetic properties and for their potential applications (permanent magnets, magnetostrictive actuators or sensors, magnetocaloric materials, high density magnetic recording, hydrogen storage ...).

RT_y compounds are intergrowth phases ($2 < y < 5$). These compounds consist of a stack of units: the R_2T_4 and RT_5, that can also represented by $[A_2B_4]$ and $[AB_5]$ units. RT_y compounds are polymorphic phases, i.e. for the same composition, the system presents several possible structures. In this case, one obtains either the hexagonal structure (H) of space group $P6_3/mmc$ or the rhombohedral structure (R) of space group $R\bar{3}m$. This binary RT_y compounds can be described by the following equation [4, 5]: $y = (5n+4)/(n+2)$ with $n = 0, 1, 2, 3, 4 \ldots$, $n \geq 0$ is an integer representing the number of units $[AB_5]$ in an elementary brick. In a general way, whatever y is, $[A_2B_4] + n[AB_5]$ can describe the elementary brick in this type of system. Thus, $n = 1$ corresponds to the stoichiometry RT_3, $n = 2$, to the stoichiometry R_2T_7, and $n = 3$, to the stoichiometry R_5T_{19}. With the same rules, we find that $n = 0$ corresponds to the stoichiometry RT_2, while $n \to \infty$ corresponds to the stoichiometry RT_5.

The magnetocaloric effect (MCE) in various magnetic materials has been extensively investigated experimentally and also theoretically, not only because of their potential applications for active magnetic refrigeration but also for understanding the fundamental properties of these materials. The intermetallic compounds were also studied for their MCE such as $La(FeSiCo)_{13}H$, R_2Fe_{17}, and $Gd_5(GeSi)_4$ [6–19].

The RCo_3 compounds are formed for all rare earths [20], their lattice parameters decrease with the rare-earths atomic number, this is related to the contraction of the lanthanides [21] except for the special case of the $CeCo_3$ compound, where cerium has a smaller size than other rare earths [22].

Very few studies were devoted to magnetocaloric effect for RCo_3 compounds. The majority of $R-T$ intermetallic compounds show a second order magnetic transition (SOMT) [17, 23–26]. However, the compounds that possess a SOMT exhibit negligible loss by thermal and magnetic hysteresis, which is a definite advantage for magnetic refrigeration.

In this work, we focused on the structural and magnetic properties of the intermetallic compound $PrCo_3$ prepared by high energy ball milling followed by a short heat treatment. We chose this compound because it has several potential advantages: (i) it is low cost and has better corrosion resistance than Gd which is the ideal candidate for the magnetocaloric effect. (ii) It does not exhibit thermal or magnetic hysteresis since it has a second order magnetic transition. (iii) In addition, this compound is a multifunctional material (magnetically hard, good hydrogen storage capacity and good magnetocaloric properties).

The crystal structure of this compound was found an inter-growth of $MgZn_2$ and $CaCu_5$ stacked structures. Furthermore, for the first time we studied the low-field magnetocaloric properties of the rhombohedral $PrCo_3$ $PuNi_3$-type compound.

* Corresponding author: bessais@icmpe.cnrs.fr

II. EXPERIMENT

$PrCo_3$ samples were prepared by melting praseodymium (99.9 wt%) and cobalt (99.9 wt%) in appropriate stoichiometric proportions. A small excess of Pr was accounted for, in order to compensate some losses due to the volatile nature of the rare earth. The melting process was done by an electric arc furnace equipped with a W electrode under high-purity Ar atmosphere. In this process, the ingots obtained were remelted five times to achieve a better homogenization of the material.

The ingots were then subsequently processed into nanopowders by undergoing high energy ball milling for 5 hours in Ar atmosphere, using a Fritsch P7 planetary mill. The resulting powder was then wrapped in tantalum sheets and vacuum-sealed in a silica tube. Finally, the sealed tube was then placed in a furnace and heated at 1000° C for 30 minutes. The thermal treatment was interrupted by quenching in cold water.

To identify the phases and describe the cell parameters of our compound, X-ray powder diffraction was carried out on a BRUKER diffractometer using Cu Kα radiation (λ = 1.5405 Å) with an internal silicon standard in order to insure an accuracy of $\pm 10^{-3}$ Å for the unit-cell parameter. The intensities were measured at angles ranging from $2\theta = 20°$ to 80° with a step size of 0.015°. The Rietveld refinement of the diffractograms where then carried out using the FullProf computer code [27, 28] in the supposition of the Thompson-Cox-Hastings line profile which allows the multiple-phase refinement in case of coexisting phases. The size of the diffraction domain in the sample was determined from the line pattern broadening, using the formula of Scherrer. The best refinement fit agreement is given by the usual agreement factors R_B and χ^2 [3, 29].

All the magnetic measurements such as Curie temperature T_C and isothermal magnetic curves $M(H)$ were measured on a differential sample magnetometer MANICS in fields up to 15 kOe, on 10 mg powder samples.

III. RESULTS AND DISCUSSION

A. Structure analysis

It is important to emphasize that the structure of the $PrCo_3$ phase with a $PuNi_3$-type structure is described by the stacking along the c-axis of the unit blocks $PrCo_2$ ($MgCu_2$) and $PrCo_5$ ($CaCu_5$) [30]. The AB_3 unit blocks are obtained by stacking the A_2B_4 and AB_5 unit blocks three times. The block cell contains two non-equivalent crystallographic sites: Pr atoms in $3a$ and $6c$ sites, whereas, Co atoms in $3b, 6c$ and $18h$ sites.

X-ray diffractograms were refined using the FULLPROF program with the Rietveld method using a Thompson-Cox-Hastings-pseudo-Voigt peak shape function [31–33]. As a measure of refinement quality, two factors of agreement R_B and χ^2 were used. The parameters of the unit cell were derived with Si standard ($a = 5.4308$ Å) leading to an accuracy of the unit cell parameters of $\pm 1.10^{-4}$ Å [34, 35].

Table I. Unit cell parameters of the rhombohedral $PrCo_3$ compound of $PuNi_3$ type structure, space group $R\bar{3}m$.

Parameters	value
a(Å)	5.0783(5)
c(Å)	24.7943(9)
$z(6c)$Pr	0.1408(3)
$z(6c)$Co	0.3331(5)
$x(18h)$Co	0.4965(4)
$y(18h)$Co	0.5034(6)
$z(18h)$Co	0.0802(4)
c/a	4.8915
V(Å)^3	551.417(2)
R_B	5.2
χ^2	3.1

Fig. 1 shows the profile fit using the Rietveld analysis for the $PrCo_3$ compound. These results show that the sample is a single-phase with around 1% of a secondary phase. The diffraction peaks are indexed in the rhombohedral $R\bar{3}m$ space group (PuNi3-type structure).

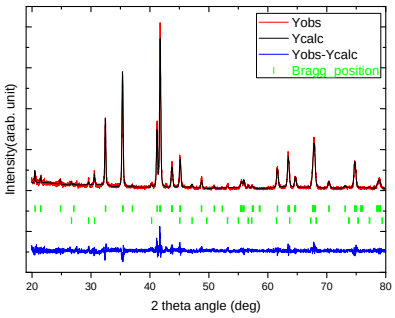

Figure 1. The Rietveld refinement of $PrCo_3$

In the table I, we have listed the best values of R_B and χ^2. The unit cell parameters (a= 5.0783(5) Å and c= 24.7943(9) Å) for $PrCo_3$ are in good agreement with the results found in the literature [36]. The atomic positions (x, y, z) and the occupation of the different Wyckoff positions of the compound $PrCo_3$ are grouped in table I.

B. Magnetic and magnetocaloric properties

1. *Thermomagnetic properties*

In this part, we will focus on intrinsic and extrinsic magnetic properties. The Curie temperature T_C, is the intrinsic magnetic order transition. In intermetallics, constituted by rare-earth-transition-metal alloys, the magnetic transition temperature depends on

three types of exchange interactions. The exchange interaction $3d-3d$ ($J_{\text{Co-Co}}$) between the moments of the Co sublattice, and the $4f-4f$ (Exchange ($J_{\text{Pr-Pr}}$)) and the intersublattice $3d-4f$ exchange interaction ($J_{\text{Pr-Co}}$)). We note that the $4f-4f$ rare earth interaction is expected to be low and negligible in comparison compared to the other two types of exchange interactions [37, 38].

The temperature dependency of the magnetization (Fig. 2) shows that T_C is equal to 330 K determined by the calculation of the minima of the dM/dT derivative. This para- to ferromagnetic transition is due essentially to the predominance of the positive Co-Co exchange interactions $3d-3d$ [37, 38].

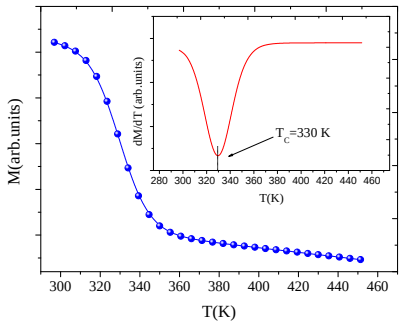

Figure 2. Magnetization as a function of temperature for the PrCo3 compound. The T_C is determined by the derivation method. The inset representation dM/dT vs. temperature

2. *Phenomenological approach*

To determine the MCE in the magnetic material $PrCo_3$, a phenomenological model is used to simulate magnetization vs temperature curve, under a low magnetic field within the adiabatic conditions. It was demonstrated by the mean field theory that the magnetisation dependence on the temperature and on T_C is given by [39]:

$$M(T) = \frac{M_{\text{fer}} - M_{\text{par}}}{2}\tanh\left[\delta(T_C - T)\right] + T\frac{dM}{dT}|_{T<T_C} + \gamma \tag{1}$$

where M_{fer} is an initial magnetization value at the ferro-paramagnetic transition for $T < T_C$ and M_{par} is a final value of magnetization at the ferro-paramagnetic transition for $T > T_C$. δ and γ parameters are given by the following two equations:

$$\delta = \frac{2(\frac{dM}{dT}|_{T<T_C} - \frac{dM}{dT}|_{T_C})}{M_{\text{fer}} - M_{\text{par}}}$$

$$\gamma = \frac{M_{\text{fer}} + M_{\text{par}}}{2} - \frac{dM}{dT}|_{T<T_C}.T_C$$

where $\frac{dM}{dT}|_{T<T_C}$ represent the sensitivity of magnetization $\frac{dM}{dT}$ at ferromagnetic state and $\frac{dM}{dT}|_{T_C}$ is magnetization sensitivity $\frac{dM}{dT}$ at T_C. Under adiabatic condition, the magnetic entropy change can be obtained by the integration of magnetization derivative as follow:

$$\begin{aligned}\Delta S_M = &-\delta.H_{max}\frac{M_{\text{fer}} - M_{\text{par}}}{2}sech^2[(\delta(T_C - T))] \\ &+ (\frac{dM}{dT}|_{T<T_C}).H_{max}\end{aligned} \tag{2}$$

Eq. 2 Shows that an observed relatively large magnetic entropy change is a consequence of high magnetization at ferromagnetic state and rapid drop in magnetization at $T = T_C$. Hence, the peak of the magnetic entropy change ΔS_M^{max} can be calculated using the equation Eq. 2, in fact, for $T_C = T$ ΔS_M=ΔS_M^{max}, so, it is expressed as follow:

$$\Delta S_M^{max} = (-\delta\frac{(M_{\text{fer}} - M_{\text{par}})}{2} + (\frac{dM}{dT}|_{T<T_C}))H_{max}$$

The specific heat can be deduced from ΔS_M, using the relation below[**?**]:

$$\Delta C_p = T\frac{\delta\Delta S_M}{\delta T}$$

Based on the above formula, heat capacity change $\Delta\delta C_p$, can be expressed as:

$$\begin{aligned}\Delta C_p = &-\delta^2.H_{max}.T\frac{M_{\text{fer}} - M_{\text{par}}}{2}sech^2[(\delta(T_C - T))] \\ &\times \tanh[\delta(T_C - T)]\end{aligned} \tag{3}$$

From this phenomenological model ΔS_M^{max} and $\Delta C_{p,H}$ can be simply evaluated for $PrCo_3$ compound under magnetic field variation.

Table II. ΔS_M^{max} and $\Delta C_{p,H}$ for $PrCo_3$ at low magnetic field

Magnetic field	ΔS_M^{max} J.(kg.K)$^{-1}$	$\Delta C_{p,H}$ J.(kg.K)$^{-1}$
$\mu_0 H = 0.13\,T$	0.16	-5.1;5.27
$\mu_0 H = 0.23\,T$	0.27	8.1;8.25

Fig. 3 shows a good agreement between modeled and experimental magnetization variation with temperature for $PrCo_3$, symbols represent experimental data, and the red line corresponds to modeled magnetization.

Moreover, Fig. 4 and Fig. 5 show ΔS_M and $\Delta C_{p,H}$ variation with temperature under a tow low magnetic fields , respectively. Predicted values of ΔS_M^{max} and ΔC_p under tow relatively low magnetic field for $PrCo_3$ are determined as shown in Tab II. From Fig. 4 and Fig. 5 we can easily see that the increase of magnetic field causes an increase of ΔS_M values from $0.13\,J.(kg.K^{-1})$ to $0.27\,J.(kg.K)^{-1}$.

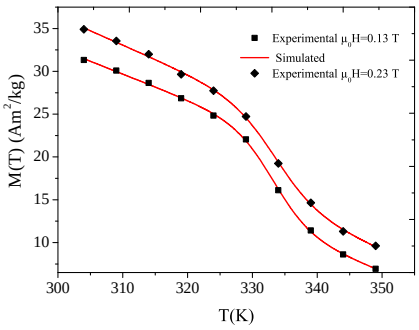

Figure 3. Magnetization vs temperature for $PrCo_3$ under tow low magnetic field.

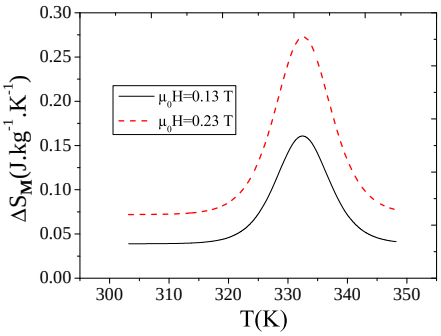

Figure 4. Modeled magnetic entropy change $(-\Delta S_M)$ versus temperature for the samples $PrCo_3$ under tow low magnetic fields.

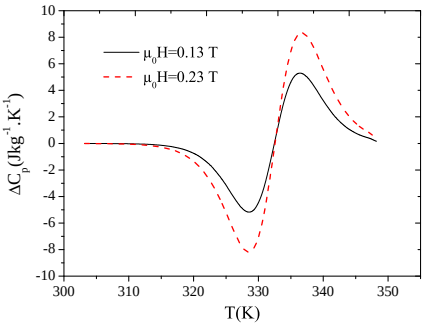

Figure 5. Change of the specific heat for $PrCo_3$ under tow low magnetic field vs temperature

3. *Experimental approach: magnetocaloric effect*

The MCE shows the isotherm entropy change. For a constant pressure, the total entropy, $S(T, H)$ is the combination of electronics $(S_{\rm el})$, magnetic (S_m), and lattice $(S_{\rm lat})$ [40]. It can be expressed as follows:

Table III. $M_{\rm fer}$ (Am^2.(kg)$^{-1}$), $M_{\rm par}$ (Am^2.(kg)$^{-1}$), $\frac{dM}{dT}|_{T<T_C}$ (Am^2.(kg.K)$^{-1}$) and $\frac{dM}{dT}|_{T_C}$(Am^2.(kg.K)$^{-1}$) determined from experimental $M(T)$ for $PrCo_3$

$\mu_0 H$ (T)	$M_{\rm fer}$	M_{par}	$\frac{dM}{dT}\|_{T<T_C}$	$\frac{dM}{dT}\|_{T_C}$
0.13	22.74	11.6	-0.299	-1.24
0.23	25.19	14.56	-0.334	-1.13

$$S(T, H) = S_m(T, H) + S_{\rm lat}(T) + S_{\rm el}(T)$$

We calculated the MCE in terms of the isothermal magnetic entropy change ΔS_M using the magnetization isotherms measured at different temperatures. For PrCo3, we determined the isothermal magnetization between 310 and 355 K, under a weak magnetic field of 1.5 T. Fig. 6 illustrates the representative isothermal magnetization curves $M(H, T)$ of the intermetallic compound, recorded at various temperatures near T_C.

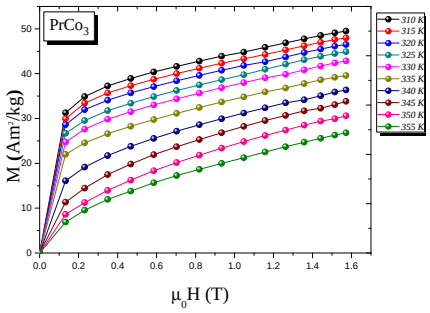

Figure 6. Isotherm magnetization curves, M(H), for PrCo3 compound.

Analysis of Arrott's plots, M^2 versus H/M, obtained from the magnetic field dependency of isothermal magnetization, is shown in figure Fig. 7. Having in mind Banarjee criterion [50], the positive slope and linear behavior near T_C confirm that the magnetic phase transition is of second order from the ferromagnetic to the paramagnetic state.

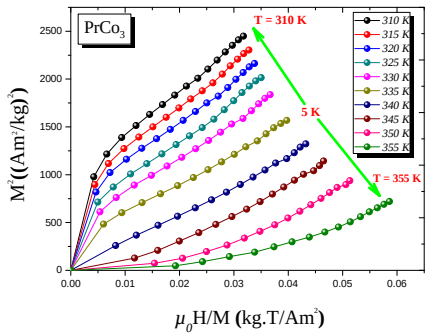

Figure 7. The Arrott plots of PrCo3 compound.

Table IV. Summary of magnetocaloric properties of PrCo3 compound compared with other magnetic materials.

Compound	μ_0H (T)	T_C (K)	$-\Delta S_M^{max}$ J/(kg.K)	Ref.
PrCo3	1.5	330	1.3	This work
Pr_2Co_7 ($P6_3/mmc$)	1.5	600	1.1	[41]
Pr_2Co_7 (R-3m)	1.5	580	3.7	[41]
Pr_5Co_{19}	1.5	690	5.2	[42]
$Gd_2Fe_{16}Si$	1.5	522	3.07	[18]
Gd	1.5	293	3.8	[43]
Pr_2Fe_{17}	1.5	285	2	[44]
$SmNi_5$	1.5	29	1.2	[25]
SmNi	1.5	42	0.65	[45]
$GdNi_3FeSi$	1.5	168	0.5	[46]
GdNi	2	69	8.9	[47]
TbNi	2	67	11.5	[47]
DyNi	1.5	61	2	[48]
$LaFe_{11.8}Si_{1.2}$	1	186	3.1	[49]

The MCE has been investigated in terms of change in isothermal magnetic entropy ΔS_M from the magnetisation isotherms obtained around T_C. We calculate the change in magnetic entropy using Maxwell's thermodynamic relation, via this equation [51, 52]:

$$\Delta S_M(T, \Delta H) = \int_0^{\mu_0 H_{max}} \left(\frac{\partial S(T,H)}{\partial H}\right)_T dH \qquad (4)$$

From Maxwell's thermodynamic relation

$$\left(\frac{\partial S(T,H)}{\partial H}\right)_T = \left(\frac{\partial M(T,H)}{\partial T}\right)_H \qquad (5)$$

We can finally obtain the equation of magnetic entropy variation :

$$\Delta S_M(T, \Delta H) = \int_0^{\mu_0 H_{max}} \left(\frac{\partial M(T,H)}{\partial T}\right)_H dH \qquad (6)$$

Based on the magnetization isotherm data, we can obtain indirectly the MCE [53]:

$$\Delta S_M(T_i, \Delta H) = \mu_0 \sum_i \frac{M_{i+1} - M_i}{T_{i+1} - T_i} \Delta H_i \qquad (7)$$

Where μ_0 is the vacuum magnetic permeability, and M_i, M_{i+1} are the magnetization values measured at T_i and T_{i+1} in a field change of ΔH_i [53]. From these calculations, we deduce the evolution of ΔS_M with temperature and applied field. Fig. 8 represents the thermal variation of magnetic entropy change of PrCo3 compound. The $-\Delta S_M^{max}$ increases with temperature evolution. $-\Delta S_M^{max}$ value is reached at $T = T_C$. The maximum value is about 1.3 J/(kg.K) under a magnetic field of 0-1.5 T. It's important to note that the $-\Delta S_M^{max}$ is high compared to other materials for magnetic refrigeration, such as Pr_2Fe_{17} ($\Delta S = 2$ J/(kg.K), μ_0H = 1.5 T) [44], $SmNi_5$ ($\Delta S = 1.2$ J/(kg.K), μ_0H = 1.5 T) [25] and $GdNi_3FeSi$ ($\Delta S = 0.5$ J/(kg.K), μ_0H = 1.5 T) [46].

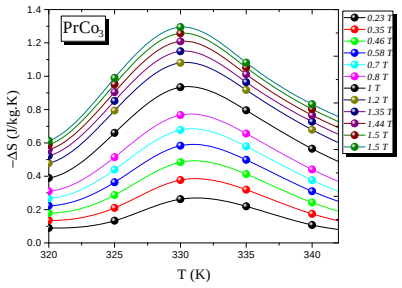

Figure 8. Magnetic entropy change ΔS_M versus temperature around the Curie temperature for PrCo3 compound

Table IV summarize the maximum in entropy change $-\Delta S_M^{max}$, Curie temperature and applied field for different intermetallic compound, developed for MCE application. The relative cooling power (RCP) is the second parameter for MCE characterization. We can deduce RCP, by application of the following equation based on magnetic entropy change [54, 55]:

$$RCP = -\Delta S_M \delta T_{FWHM} \qquad (8)$$

The RCP is equal to 21 J/kg for the intermetallic PrCo3. Let's notice that, the high magnetic entropy change and the larger δT can provide a high RCP value.

In order to compare the predicted magnetic entropy change using the phenomenological approach and the magnetic entropy change obtained by experimental approach, both curves are plotted on the same figure. Fig .9

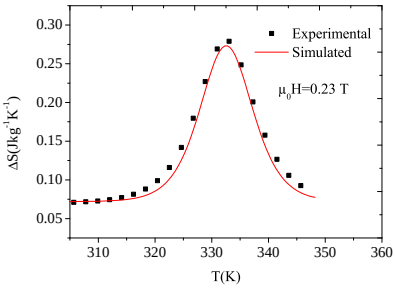

Figure 9. Phenomenological ΔS_M versus experimental one around the Curie temperature for PrCo3 compound

shows a good agreement between the two approaches, based on this result, the phenomenological model can be used to predict and describe the MCE of the intermetallic compounds.

IV. CONCLUSION

In this work we demonstrated that by using arc melting, $PrCo_3$ samples can be obtained faster than with other synthesis methods. The pure nanocrystalline phase $PrCo_3$ is finally obtained with a process consisting of high energy ball milling followed by a short heat treatment.

Rietveld refinement of XRD data confirmed the crystallization of the compound into rhombohedral $PuNi_3$ type structure (space group $R\bar{3}m$). The rare earth Pr atoms occupy both $3a$ and $6c$ crystallographic sites, whereas the Co atoms are placed on the sites $3b$, $6c$ and $18h$.

We also report new magnetic and magnetocaloric properties obtained for the first time for the nanocrystalline $PrCo_3$: it exhibits a Curie temperature of 330 K and a maximum in entropy variation of 1.3 J/kg.K. From these measurements we also deduced its relative cooling power, which is approximately equal to 21 J/kg. We have deduced from the Arrott plots that the nature of its ferromagnetic to paramagnetic transition is of second order.

In addition, a theoretical approach was used that permit to successfully predict ΔS_M , using a faster indirect method that delivers important information about the magnetocaloric properties of $PrCo_3$ compound. Due to its magnetic transition near ambient temperature, $PrCo_3$ can be a potential candidate, that could be optimized by targeted substitution to exhibit a large magnetocaloric effect.

DECLARATIONS

Declaration of interests

The authors declare that they have no known competing financial interests or personal relationships that could have appeared to influence the work reported in this paper.

Data availability

All data generated or analyzed during this study are included in this published article .

Author Contributions

All authors contributed to the study conception and design. Material preparation, data collection and analysis were performed by S. Ayadim, H. Jaballah, W. Bouzidi, K. Nouri and T. Bartoli. The first draft of the manuscript was written by W. Bouzidi, K. Nouri, T. Bartoli and all authors commented on previous versions of the manuscript. All authors read and approved the final manuscript.

Funding

The authors did not receive support from any organization for the submitted work.

Conflicts of interests

The authors have no relevant financial or non-financial interests to disclose.

The authors have no competing interests to declare that are relevant to the content of this article.

[1] B. D. Cullity, *Introduction to Magnetic Materials* (Addison-Wesley Publishing Company, Reading, Massachusetts, 1972).
[2] J. M. D. Coey and H. Sun, J. Magn. Magn. Mater. **87**, L251 (1990).
[3] L. Bessais and C. Djega-Mariadassou, Phys. Rev. B **63**, 54412 (2001).
[4] Y. Khan, Acta. Crystallogr. **30**, 1533 (1974).
[5] Y. Khan, Phys. Stat. Sol. **23**, 425 (1974).
[6] V. K. Pecharsky and K. A. Gschneidner, J. Magn. Magn. Mater. **167**, L179 (1997).
[7] V. K. Pecharsky and K. A. Gschneidner, Phys. Rev. Lett. **78**, 4497 (1997).
[8] K. A. Gschneidner, V. K. Pecharsky, E. Bruck, H. G. M. Duijin, and E. M. Levin, Phys. Rev. Lett. **85**, 4190 (2000).
[9] S. Fujieda, A. Fujita, and K. Fukamichi, Appl. Phys. Lett. **81**, 811276 (2002).

[10] H. Tang, V. K. Pecharsky, G. D. Samolyuk, M. Zou, K. A. Gschneidner, V. P. Antropov, D. L. Schlagel, and T. A. Lograsso, Phys. Rev. Lett. **93**, 237203 (2004).

[11] S. Fujieda, A. Fujita, and K. Fukamichi, J. Magn. Magn. Mater. **310**, e1004 (2007).

[12] H. Chen, Y. Zhang, J. Han, H. Du, C. Wang, and Y. Yang, J. Magn. Magn. Mater. **320**, 1382 (2008).

[13] A. Fujita, S. Fujieda, and K. Fukamichi, J. Magn. Magn. Mater. **321**, 3553 (2009).

[14] P. Gorria, P. Alvarez, J. S. Marcos, J. Sanchez-Llamazares, M. J. Perez, and J. A. Blanco, Acta Mater. **57**, 1724 (2009).

[15] M. Phejar, V. Paul-Bancour, and L.Bessais, Intermetallics **18**, 2301 (2010).

[16] S. Charfeddine, K. Zehani, L. Bessais, and A. Korchef, **238**, 15 (2016).

[17] V. Franco, J. S. Blazquez, J. J. Ipus, J. Y. Law, L. M. Moreno-Ramirez, and A. Conde, Prog. Mater. Sci. **93**, 112 (2018).

[18] K. Nouri, T. Bartoli, A. Chrobak, J. Moscovici, and L. Bessais, Journal of Electronic Materials **47**, 3836 (2018).

[19] S. Nikitin, N. Pankratov, A. Smarzhevskaya, J. Cwik, Y. Koshkid'ko, A. Karpenkov, D. Karpenkov, Y. P. YG Pastushenkov, K. Nenkov, and K. Rogacki, J. Alloys Compd. **854**, 156214 (2021).

[20] R. Lemaire, Cobalt **33**, 201 (1966).

[21] R. Lemaire, R. Pauthenet, J. Schweizer, and I. S. Silvera, J. Phys. Chem. Solids **28**, 2471 (1967).

[22] V. V. Burnasheva, V. V. Klimeshin, V. A. Yartys, and K. N. Semenenko, Inorg. Mater. **15**, 627 (1979).

[23] R. Guetari, R. Bez, A. Belhadj, K. Zehani, A. Bezergheanu, N. Mliki, L. Bessais, and C. Cizmas, J. Alloys Compd. **588**, 64 (2014).

[24] R. Guetari, T. Bartoli, C. B. Cizmas, N. Mliki, and L. Bessais, J. Alloys Compd. **684**, 291 (2016).

[25] K. Nouri, M. Jemmali, S.Walha, K. Zehani, A. B. Salah, and L. Bessais, J. Alloys Compd. **672**, 440 (2016).

[26] W. Bouzidi, K. Nouri, T. Bartoli, R. Sedek, H. Lassri, J. Moscovici, and L. Bessais, J. Magn. Magn. Mater. **497**, 166018 (2020).

[27] J. Rodriguez-Carvajal, M. Fernandez-Diaz, and J. Martinez, J. Phys.: Condens. Matter **81**, 210 (1991).

[28] J. Rodriguez-Carvajal, Physica B **55**, 192 (1993).

[29] C. Djega-Mariadassou and L. Bessais, J. Magn. Magn. Mater. **210**, 81 (2000).

[30] K. Younsi, V. Russier, and L. Bessais, J. Appl. Phys. **107**, 8 (2010).

[31] H. Rietveld, Acta Crystallogr **22**, 151 (1967).

[32] P. Thompson, D. Cox, and J. Hasting, J. Appl. Crystallogr **20**, 79 (1987).

[33] L. Bessais, K. Younsi, S. Khazzan, and N. Mliki, Intermetallics **19**, 997 (2011).

[34] K. Zehani, R. Bez, A. Boutahar, E. Hlil, H. Lassri, J. M. N. Mliki, and L. Bessais, J. Alloys Compd. **591**, 58 (2014).

[35] N. Hosni, K. Zehani, T. Bartoli, and L. B. H. Maghraoui-Meherzi, J. Alloys Compd. **694**, 1295 (2017).

[36] K. Iwase, K. Mori, S. Shimizu, S. Tashiro, and T. Suzuki, Int. J. Hydrogen Energy **41**, 14788 (2016).

[37] E. Belorizky, M. Fremy, J. Gavigan, D. Givord, and H. Li, J. Appl. Phys. **61**, 3971 (1987).

[38] J. J. M. Franse and R. J. Radwanski, *Handbook of magnetic materials* (Elsevier, 1993).

[39] M. A. Hamad, Phase Transit. **85**, 106 (2012).

[40] A. M. Tishin and Y. I. Spichkin, *The magnetocaloric effect and its applications*, edited by IOP (Bristol, 2003).

[41] R. Fersi, W. Bouzidi, N. Mliki, and L. Bessais, Intermetallics **100**, 181 (2018).

[42] W. Bouzidi, N. Mliki, and L. Bessais, J. Electron. Mater **47**, 2776 (2018).

[43] J. Shen, J.-F. Wu, and J.-R. Sun, J. Appl. Phys. **106**, 083902 (2009).

[44] K. Zehani, R. Guetari, N. Mliki, and L. Bessais, Physics Procedia **75**, 1435 (2015).

[45] H. Drulis, A.Hackemer, A.Zaleski, Yu.L.Yaropolov, S.A.Nikitin, and V.N.Verbetsky, Solid StateCommun **151**, 1240 (2011).

[46] A. V. Morozkin, A. V. Knotko, V. O. Yapaskurt, J. Yao, F. Yuan, Y. Mozharivskyj, R. Nirmala, S. Quezado, and S. K. Malik, Journal of Solid State Chemistry **232**, 150 (2015).

[47] R. Rajivgandhi, J. A. Chelvane, S. Quezado, S. Malik, and R. Nirmala, J. Magn. Magn. Mater. **433**, 169 (2017).

[48] R. Rajivgandhi, J. A. Chelvane, A. K. Nigam, J.-G. Park, S. K. Malik, and R. Nirmala, J. Magn. Magn. Mater. **418**, 9 (2016).

[49] J. J. Ipus, J. M. Borrego, L. M. Moreno-Ramirez, J. S. Blazquez, V. Franco, and A. Conde, Intermetallics **84** (2017).

[50] B. K. Banerjee, Phys. Lett. **2**, 16 (1964).

[51] V. K. Pecharsky and K. A. Gschneidner, Magnetocaloric effect from indirect measurements: Magnetization and heat capacity, J. Appl. Phys. **86**, 565 (1999).

[52] F. X. Hu, B. G. Shen, J. R. Sun, Z. H. Cheng, and X. X. Zhang, J. Phys.: Condens. Matter **12:L691**, 6 (2000).

[53] M. Foldeaki, R. Chahine, and T. K. Bose, J. Appl. Phys. **77**, 3528 (1995).

[54] D. T. K. Anh, N. P. Thuy, N. H. Duc, T. T. Nhien, and N. V. Nong, J. Magn. Magn. Mater. **262**, 427 (2003).

[55] M. Balli, M. Rosca, D. Fruchart, and D. Gignoux, J. Magn. Magn. Mater. **321**, 123 (2009).